Characterization and Comparison of Carbide and Phase Evolution in Intermediate Nickel Alloys

Student Names: Yixuan Ding, Krish Gupta, Jackie Lane, Nathan Robinson, Mitchell Weber
Faculty Advisors: Dr. Maria Okuniewski
Industrial Sponsors: Dianna Clute, Walter Isenburg, Mike Pollard, Chad Miller

PURDUE UNIVERSITY
School of Materials Engineering

The engine valves made from Caterpillar's nickel-based alloy are designed to function during prolonged exposure to high temperatures, with intense oxidation and corrosion risks. During service, carbide precipitates begin to form due to heat aging, which is encouraged to strengthen the material properties of the valves, but can also potentially cause failure in these expensive alloys. This project investigates heat aging of these specific engine valves, utilizing diverse experimental methodologies to investigate the carbide evolution, phase changes within the alloy, and physical property changes during the heat aging process, thus offering a detailed characterization of the alloy's behavior during heat aging.

This work is sponsored by Caterpillar Inc, West Lafayette, IN

CATERPILLAR®

Background & Objectives

Background

Crutonite and VAT-36 are intermediate iron nickel superalloys used for exhaust and intake valves, shown in green in Fig 1, in diesel and natural gas combustion engines. These alloys are chosen for their high corrosion resistance and strength for making them preferable for intense environments.

These valves face extreme temperatures while in use, some going above the recrystallization temperature of 747° C, as shown in Figure 2. This could result in microstructural changes that influence the integrity of the mechanical properties and result in premature failure or degradation that could pose issues to the customer.

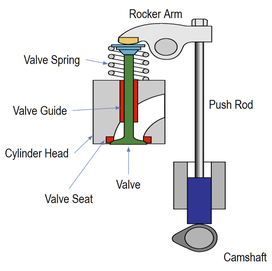

Figure 1: Engine system that includes the valves (green)

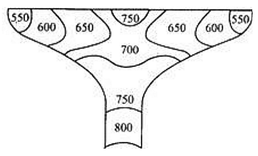

Figure 2: Temperature range (°C) seen in use of exhaust valves [1]

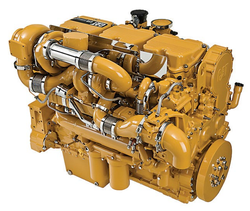

Figure 3: Example Caterpillar engine

Purpose of Project:
Caterpillar is looking to understand the behavior of both alloys over different times and temperatures, specifically looking at the microstructural changes of various precipitates and phases. This information will then be taken and connected to the changes in the mechanical properties to understand the lifecycle of the valves.

Chemistry Background

Table 1: Crutonite [2] and VAT-36 [3] chemical composition in wt%

Alloys/Elem	Cr	Si	Nb	Ti	Al	Ni	Fe
Crutonite	15-20	0.15	1.8-2.5	2.0-3.5	1.63-2.3	30-35	Bal.
VAT-36	19	NA	2	1.20	1.95	36	Bal.

Experimental Procedure

Specimen Preparation

- Taking two valves each of Crutonite and VAT-36, stems were separated to focus on the valve base. The base was cut into 8 pieces as shown in Fig. 3.

Heat Aging

- One control sample was set aside for each alloy type and 7 experimental samples for each temperature setting, as shown in Table 1("C" for Crutonite, "V" for Vat-36). Two temperatures, 750℃ (designated as "L" in Table 1, means low temperature) and 840℃ (designated as "H" in Table 1, means high temperature), were chosen to represent the temperature range seen in use and to check for possible recrystallization, phase changes and physical property changes. Every 96 hours (4 days as one interval), one sample was removed for each alloy up to 672 hours (28 days) and labeled as how many intervals of time the samples are heat aged.

Scanning Electron Microscopy (SEM) / Energy-dispersive X-ray spectroscopy (EDS)

- SEM and EDS analysis gave insight into the phases and carbides in the microstructure and their specific chemistry. Only the controls and sets 1, 4, and 7 were analyzed for each alloy and temperature setting. Images are taken on the upper curve and bottom edge, with EDS applied on the bulk for composition analysis.

X-Ray Diffraction (XRD)

- XRD analysis gives information on the crystallography of the phases and carbides. XRD will additionally reaffirm the phase identification and carbide analysis findings done prior. Only the controls and sets 1, 4, and 7 were tested. Each sample was tested under parameters of a scanning speed of 3 degrees/minute and a divergence slit of 2.9 mm on a Bruker X-Ray Diffractometer.

Hardness

- The samples were tested using the Vickers hardness scale. Values were used to connect microstructural changes over time and temperature to mechanical property trends and relate to literature values.

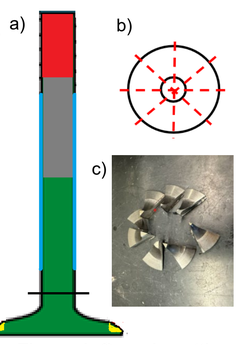

Figure 4: Sample cutting demonstrations (a, b) and results (c)

Table 2: Labelling scheme for heat aged samples with time

	Crutonite		VAT 36	
96 hrs	CL1	CH1	VL1	VH1
192 hrs	CL2	CH2	VL2	VH2
288 hrs	CL3	CH3	VL3	VH3
384 hrs	CL4	CH4	VL4	VH4
480 hrs	CL5	CH5	VL5	VH5
576 hrs	CL6	CH6	VL6	VH6
672 hrs	CL7	CH7	VL7	VH7

Optical Microscopy

Optical micrographs were taken to observe material phase changes, appearance changes and any other evident changes between the different aging temperatures and times for each alloy such as decarburization and banding.

Results - Microstructure & Phase

Scanning Electron Microscopy / Energy-Dispersive X-ray Spectroscopy - Phase Changes & Growth During Aging

Primary Phases

- Before aging, VAT-36 microstructure is observed to contain primary titanium (Ti)-based carbides and niobium (Nb)-based carbides.
- Crutonite contains Ti-based and Nb-based primary carbides. There are also both large and intergranular NbSi-rich phases.

Growth of Intergranular Phases

- As VAT-36 is aged at 750 °C, an intergranular Cr-rich phase grows over time while the NbSi-rich phase grows minimally. At 840 °C, the NbSi-rich phase appears immediately and grows heavily with minimal growth of the Cr-rich phase.
- In Crutonite, the NbSi-rich phase appears unchanged at 750 °C but grows quickly and then plateaus at 840 °C.
- The NiTiAl-rich phase (gamma prime) grows and appears at both temperatures, although it shows much greater growth at 840 °C than 750 °C.

The preference for different phases to form at higher and lower temperatures can inform the time and temperature the valve has been exposed to in-service, while also explaining mechanical behavior

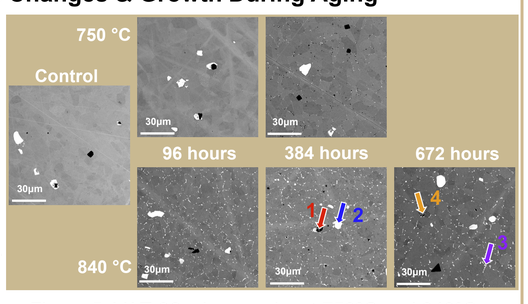

Figure 5: VAT-36 micrographs at 750°C and 840°C.

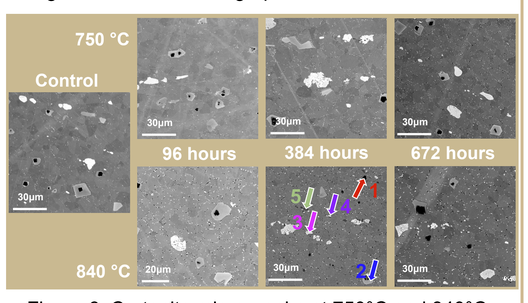

Figure 6: Crutonite micrographs at 750°C and 840°C.

Table 3: EDS spot scans of VAT-36 and Crutonite showing compositions in wt.%.

	VAT-36				Crutonite				
Element Symbol	Spot 1	Spot 2	Spot 3	Spot 4	Spot 1	Spot 2	Spot 3	Spot 4	Spot 5
Ni	3.86	3.26	25.08	25.06	3.14	2.02	15.46	14.39	48.02
Fe	4.5	3.69	34.27	25.15	---	4.63	31.24	32.19	11.57
Ti	85.05	14.98	1.19	1.15	75.38	29.07	5.24	5.37	15.01
Nb	3.49	74.56	20.25	1.23	17.79	61.06	27.67	27.26	2.5
Cr	2.66	2.16	15.76	45.50	2.57	1.69	8.89	9.36	3.18
O	---	---	---	---	---	---	7.04	7.63	5.48
C	0.43	1.34	---	---	1.13	1.53	---	---	---
Al	---	---	1.51	1.92	---	---	1.79	1.10	14.25
Si	---	---	1.95	---	---	---	2.68	2.70	---

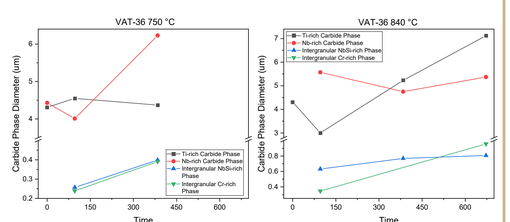

Figure 7: Carbide and intergranular phase size transformations with time for VAT-36

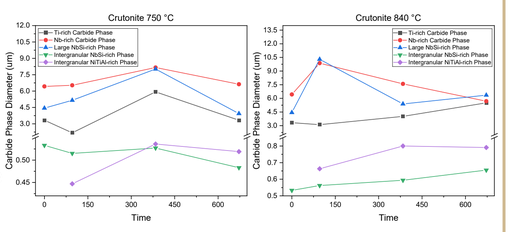

Figure 8: Carbide and intergranular phase size transformations with time for Crutonite

X-Ray Diffraction

- Identified FCC nickel, BCC iron, gamma (γ), and gamma prime (γ') phases, as expected per literature [4], through Bragg's law calculations
- Intergranular phases identified at 2Θ = 36° in aged samples only
- Peak splitting in the large peak at 2Θ = 43° observed from the different crystallographic phases found in the microstructure, particularly in Crutonite
- Peak shifts are seen between the controls and 96 hours, indicating a change in crystallography and phases
- Peaks representing γ and γ' in Figure 9 are seen growing in intensity with time
- The intergranular (IG) phases appear more in the Crutonite than in the VAT-36

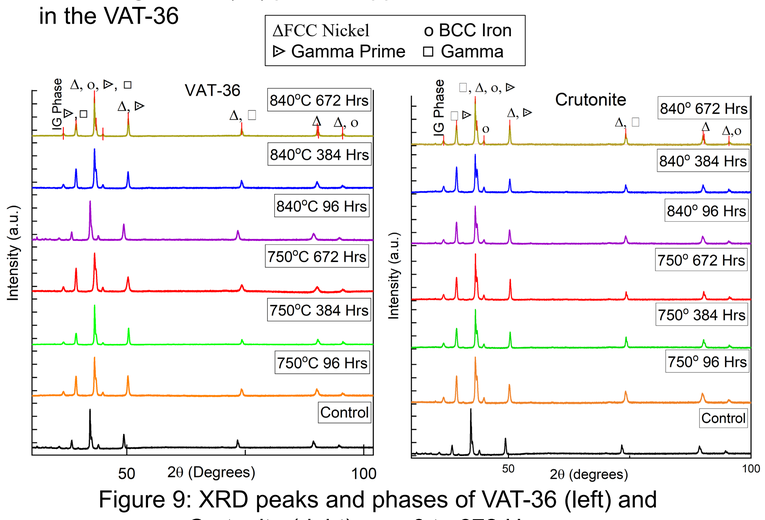

Figure 9: XRD peaks and phases of VAT-36 (left) and Crutonite (right) over 0 to 672 Hours

Results - Mechanical Behavior

Optical Microscopy – Decarburization, Deformation, and Banding

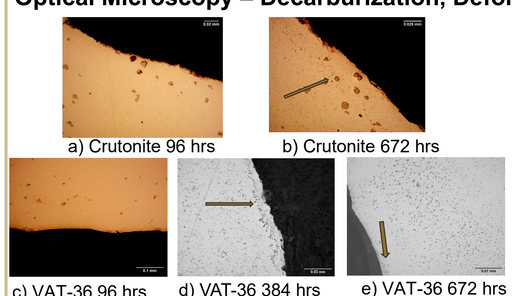

Figure 11: Optical micrographs of decarburization with 840°C

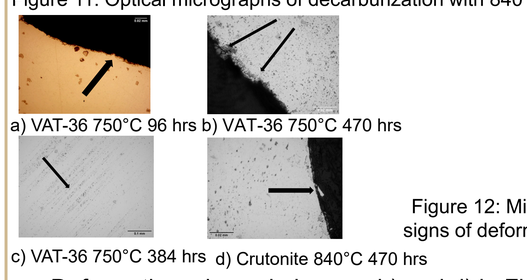

Figure 12: Micrographs showing signs of deformation and banding.

- Samples tested under higher temperatures for both samples began to show signs of decarburization. Decarburization could result in reduced strength and the identified decrease in hardness. The arrows in Figure 11 represent the areas of decarburization.
- Deformation, shown in images b) and d) in Figure 12, are observed along the surfaces of aged samples, with whole sections fracturing off at times. This degradation of the integrity of the surface is possibly caused by a combination of oxidation, decarburization, and other factors. Also, in image c) in Figure 12, banding, or evidence of non-homogenous distribution of alloying elements, is observed.

Hardness and Microstructural Changes

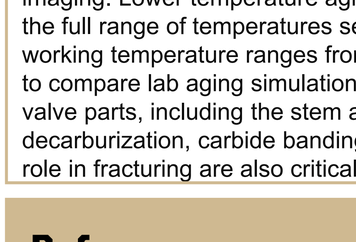

Figure 10: Vickers hardness as aging time progresses for the experimental samples versus literature data [5].

- Aging the alloys at high temperature sharply decreases hardness before decreasing steadily and plateauing, while low temperature initially increases hardness before decreasing and plateauing, demonstrating the impact of different use-case temperatures on mechanical behavior.
- The changes in hardness can be connected to the carbide evolution and phase changes shown in Figs 5 and 6. The initial appearances of the intergranular phases have a drastic impact on hardness, and the continued slow growth of these phases decreases hardness slowly.

Conclusion & Future Work

Conclusions

VAT-36 and Crutonite feature two intergranular phases that grow with temperature and time. VAT-36 develops Ti and Nb based intergranular phases, while Crutonite's Ni(Ti,Al)-based gamma prime phase expands. Gamma prime is associated with an increase in hardness, while the intergranular phases decrease hardness. These changes, influenced by heat treatment, impact properties like hardness and deformation possibility, and these might contribute to change in the performance and durability of the materials in their respective applications. Crutonite maintains a consistent higher strength than VAT-36 and therefore may be preferable for use.

Future Recommendations

To observe further phase formation, extended aging times are required, alongside high-resolution EDS for better intergranular phase imaging. Lower temperature aging should also be explored to cover the full range of temperatures seen in use based on engine valve working temperature ranges from literature. It would also be beneficial to compare lab aging simulations with actual wear data, examining all valve parts, including the stem and coating. Investigations into decarburization, carbide banding effects, and surface deformation's role in fracturing are also critical for material performance.

References

[1] Soegoto1, E. S., & Tjokroadiponto2, S. (2018, August 1). *IOPscience*. IOP Conference Series: Materials Science and Engineering. https://www.researchgate.net/figure/Temperature-fields-inside-a-exhaust-valve-5_fig2_307615254

[2] Pierce, D., Haynes, A., Hughes, J., Graves, R., Maziasz, P., Muralidharan, G., Shyam, A., Wang, B., England, R., & Daniel, C. (2019). High temperature materials for heavy duty diesel engines: Historical and future trends. *Progress in Materials Science*, *103*, 109–179. https://doi.org/10.1016/j.pmatsci.2018.10.004

[3] Carvalho, M. R. D. D., Antonialli, A. Í. S., & Diniz, A. E. (2020). A machinability evaluation based on the thermal and mechanical properties of two engine valve steels. *The International Journal of Advanced Manufacturing Technology*, *110*(11–12), 3209–3219. https://doi.org/10.1007/s00170-020-06108-w

[4]Awais, M., Hixson, W. R., Victor, Q., O'Neal, C., Ilavsky, J., & Coakley, J. (2023). Microstructure Evolution of a Multimodal Gamma-Prime Ni-Based Superalloy Characterized by In Situ Diffraction. *Metallurgical and Materials Transactions A*, *54*(6), 2311–2319. https://doi.org/10.1007/s11661-023-07013

[5] de Cicco, H., Luppo, M. I., Gribaudo, L. M., & Ovejero-García, J. (2004). Microstructural development and creep behavior in A286 superalloy. Materials Characterization, 52(2), 85–92. https://doi.org/10.1016/j.matchar.2004.03.007